Full-length paper

The effect of the signal-to-noise ratio in CBED patterns on the accuracy of lattice parameter determination

Andrey Chuvilin[1,*], Thomas Kups[1] and Ute Kaiser[1]

Institut für Festkörperphysik, Friedrich-Schiller-Universität Jena, Max-Wien-Platz 1, D-07743 Jena, Germany
[1]Present address: Zentrum für Mikro- und Nanotechnologien, Kirchhoffstraße 7, 98693 Ilmenau, Germany
[*]To whom correspondence should be addressed. E-mail: A.Chuvilin@microscopist.ru

Abstract A method of higher-order Laue zone line position measurement in convergent-beam electron diffraction (CBED) is proposed based on Hough transformation. A thorough analysis of the errors introduced by this measurement procedure is performed and their influence on the accuracy of lattice parameter determination is estimated. A criterion is derived which enables the accuracy to be predicted before experimental measurements are made and, thus, allows the selection of the best CBED geometry for parameter measurement.

Keywords CBED, lattice parameters measurement, HOLZ lines, measurement errors, influence of noise

Received 22 August 2003, accepted 12 March 2004

Introduction

Measurement of the higher-order Laue zone (HOLZ) line positions in convergent-beam electron diffraction (CBED) patterns of a crystalline material allows precise determination of the lattice parameters from an area of a few square nanometers. Although the method is well established and a number of measurement procedures have been suggested [1–8], estimation of the accuracy of the method is still under question. Three different approaches to estimate the measurement accuracy have been proposed to date. The first involves multiple measurements by hand on photographic prints of CBED patterns [8], with subsequent averaging of results, the deviation of results being used as an estimate of the measurement error. This approach assumes that the principal source of the error is the measurement itself and, thus, that the final accuracy is determined by the measurement procedure. The second approach is to measure a standard crystal with known lattice parameter and to state the difference between measured and tabulated values to be the error of the method [1]. This assumes that the accuracy is always the same, but this is only valid for a particular set of experimental conditions. The third approach utilizes the width and the value of the extremum of the optimization functional (e.g. the correlation maximum [1], least square functional minimum [9], etc. [8]), which is used to describe the similarity between experimental and simulated patterns. However, the above values only characterize the quality of the fit of experimental data to some particular lattice parameter set, i.e. the precision of the fit rather then the accuracy of the lattice parameter determination. The approaches mentioned either simply state the accuracy or determine it *post factum* in the process of measurement.

In this paper we introduce a method of precise HOLZ line position measurement in CBED patterns, which combines a modification of the Hough transform with the previously developed ratio method [5]. A thorough treatment of the resulting errors is given, including the influence of the signal-to-noise ratio (SNR), so that the accuracy of measurement can now be calculated a priori for each particular CBED pattern. We will not discuss here the problem of global optimization in multidimensional space (raised in [3]), as this is described in more detail in the specialist literature. Instead, we will concentrate on the case of determination of a single parameter. However, all the expressions that will be obtained can be expanded easily to the multiparameter case.

Methods

Assuming that the CBED pattern has been recorded already at well-defined experimental conditions and that the theory can correctly treat all aspects of the experiment, the task of measuring lattice parameters using HOLZ lines can be separated into two subtasks: (i) measurement of HOLZ line positions on experimental and simulated CBED patterns and (ii) then their intercomparison. The latter subtask is not straightforward, as it is necessary to deal with camera length calibration and rotational and geometrical distortions, which differ between experiment and simulation. Common practice is to compare experimental and simulated CBED patterns by measuring the distances between particular HOLZ line intersections. To exclude the need for camera length calibration and to minimize the influence of geometrical distortions, the ratios between pairs of distances rather than the distances themselves are commonly evaluated [5].

The Hough transformation was suggested [9] as a means to determine line positions and, thus, to calculate distances between intersections. The Hough transform [10] is defined by the integral operator

$$H(a, b) = \iint f(x, y)\delta[y - ax - b]dxdy$$

Thus, each straight line in (x, y) space is projected to a point in parametric (a, b) space. A line with excess (deficit) intensity profile in (x, y) space produces an intensity maximum (minimum) in (a, b) space. The position of the maximum (minimum) can then be determined using standard methods and its coordinates (a_0, b_0) are the parameters of the equation of the corresponding line. If a Hough transformation is performed on a discrete data set (digital image), the result is also discrete and the size of a pixel, $(\Delta a, \Delta b)$, in Hough space determines the uncertainty $(\pm\Delta a / 2, \pm\Delta b / 2)$ of the parameters.

The parameterization (a, b) is not the only one that can be used for Hough transformation. This parameterization has the disadvantage that for lines parallel to the y-axis, b is undefined and a is infinity; thus, a finite area of the initial data is projected onto an infinite region in Hough space. An alternative parameter set is (α, ρ), where α is the inclination angle of the line and ρ is the distance from the line to the origin. We used the latter parameter set, as it is defined without any singularities and a finite area of (x, y) space is projected onto a finite area of (α, ρ) space.

Precise measurement of a line position requires a Hough peak maximum position to be known with subpixel accuracy. Earlier [9] it was suggested to fit the Hough peak by an arbitrary analytical function and to assume the maximum of the above function to be the maximum of the peak. The accuracy was reported to be ~0.2 pixel. However, such an approach has a number of drawbacks.

(a) The shape of HOLZ lines (i.e. the shape of a corresponding Hough peak) is not exactly known, which forces the use of an empirically chosen fitting function (fourth-order two-dimensional polynomial in [9]). This in turn will give rise to a systematic error due to a probable wrong guess of the peak shape.

(b) The shape of a Hough peak is strongly influenced by the bending of the HOLZ line due to dynamical interactions and by the asymmetric background. Masking should be used to exclude the distorted parts from calculations; however, the influence of the background is difficult to eliminate.

Here, we propose achieving subpixel accuracy by subpixelation in (x, y) space (i.e. by interpolation of the original data in-between the pixels) and by performing the Hough transformation over this finer graded image. Then, the maximum of the Hough peak can be determined simply as the (sub-)pixel with maximum intensity. Local bending of a line only influences the shape of the corresponding Hough peak, but not the position of its maximum. The line position thus defined by the maximum pixel is insensitive to line bending, because it is defined in the sense of the *most probable* position of the *tip of the line profile* (i.e. the most extended straight part of the line).

The procedure of line position calculation has been developed for both speed and accuracy in the following steps.

(I) Line recognition and first approximation: a small rectangular area is selected so that the line of interest crosses this area. A Hough transformation of this area is performed, the maximum is detected and its position (α_1, ρ_1) is used as a first approximation with uncertainty $(\Delta\alpha_1, \Delta\rho_1)$.

(II) Interpolation of the region of interest: a rectangular stripe is defined along the line (α_1, ρ_1) on the CBED pattern, which covers the whole set of probable lines $(\alpha_1 \pm \Delta\alpha_1 / 2, \rho_1 \pm \Delta\rho_1 / 2)$. The dimensions of the resulting matrix are defined in order to achieve the desired final precision $(\Delta\alpha_2, \Delta\rho_2)$ and the original data are interpolated into this matrix.

(III) Final accuracy calculation: a modification of the Hough transformation is performed on this stripe, producing an $N \times M$ matrix, which covers the area $[\alpha_1 - \Delta\alpha_1 / 2 < \alpha < \alpha_1 + \Delta\alpha_1 / 2, \rho_1 - \Delta\rho_1 / 2 < \rho < \rho_1 + \Delta\rho_1 / 2]$ in (α, ρ) space. The maximum is detected and its position (α_2, ρ_2) is the final value with an uncertainty of $(\Delta\alpha_2 = \Delta\alpha_1 / N, \Delta\rho_2 = \Delta\rho_1 / M)$.

Tests show that for a noise-free line having Gaussian profile with the width of 8 pixels, length of 600 pixels and 80 grey levels, an uncertainty (hereafter referred to as the geometrical error (GErr)) of only $\Delta\alpha = 4 \times 10^{-6}$ rad, $\Delta\rho = 0.002$ pixel can be obtained. To the extent that the matrix dimensions (N, M) can be set arbitrarily, practically any predefined GErr can be achieved, limited only by computing time.

Results and discussion

Treatment of the errors

There are two different sources of errors in line position determination: the measurement procedure, which defines GErr, and the noise, which is always present in experimental images due, in particular, to finite electron statistics. Noise cuts the information content of the image and, thus, defines the principal uncertainty in the line's position. This uncertainty will be referred to as a statistical error (SErr).

Geometrical error

To simplify further discussion, we will use a scalar property ΔL to describe the GErr of a line, rather than the vector $(\Delta\alpha, \Delta\rho)$.

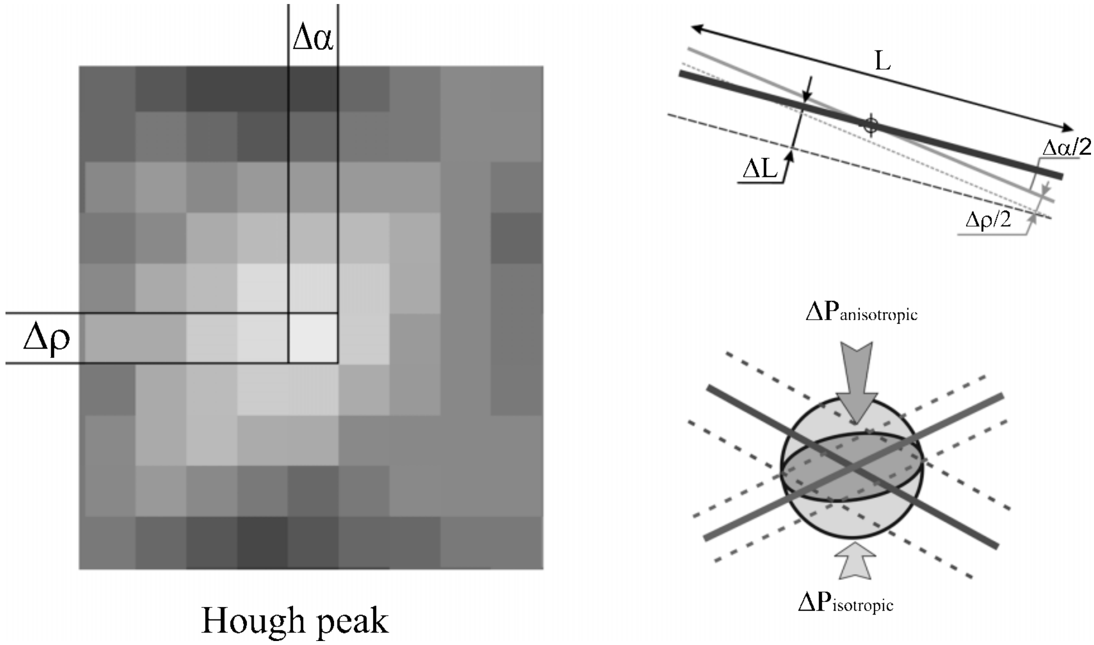

Fig. 1 Dimensions of the pixel in Hough space ($\Delta\alpha$, $\Delta\rho$) determine the uncertainty of the position ΔL of the corresponding line (eq. (1)). Uncertainty of the crossover of two lines will strongly depend on the crossing angle.

ΔL is related to the positive quadrant of the rectangular area ($\alpha \pm \Delta\alpha / 2$, $\rho \pm \Delta\rho / 2$), which contains all possible estimates of line positions (see Fig. 1).

$$\Delta L = L \sin(\Delta\alpha / 2) + \Delta\rho / 2 \tag{1}$$

where L is the length of the line within the frame of the pattern. This definition is an overestimation as the maximum error can arise only at the ends of a line (edges of the pattern). If ΔL is known, the GErr of the position of an intersection between two lines ΔP (for simplicity assumed to be isotropic) can be expressed as

$$\Delta P = \sqrt{\frac{\Delta L_1^2 + \Delta L_2^2}{\sin^2\gamma}} \tag{2}$$

where γ is the angle between two lines. The error ΔR of the ratio of two distances $R = d_1 / d_2$ is then

$$\Delta R = \frac{1}{d_2^2}\sqrt{d_1^2\left(\frac{\Delta L_1^2 + \Delta L_2^2}{\sin^2\gamma_1} + \frac{\Delta L_3^2 + \Delta L_4^2}{\sin^2\gamma_2}\right) + d_2^2\left(\frac{\Delta L_5^2 + \Delta L_6^2}{\sin^2\gamma_3} + \frac{\Delta L_7^2 + \Delta L_8^2}{\sin^2\gamma_4}\right)} \tag{3}$$

If all lines are measured to the same precision (i.e. all ΔL_i are equal), then eq. (3) can be simplified as

$$\Delta R = \frac{\sqrt{2}\Delta L}{d_2}\sqrt{\frac{d_1^2}{d_2^2}\left(\frac{1}{\sin^2\gamma_1} + \frac{1}{\sin^2\gamma_2}\right) + \left(\frac{1}{\sin^2\gamma_3} + \frac{1}{\sin^2\gamma_4}\right)} \tag{4}$$

To a good approximation there is a linear dependence between R-values and lattice parameter A (or accelerating voltage of a transmission electron microscope)

$$A = {}^{1}\!/\!_{D} \cdot R + b \tag{5}$$

where D (in nm^{-1} or kV^{-1}) is the *sensitivity* of the ratio R to variations in A. The corresponding expression for the error of A is then

$$\Delta A = {}^{1}\!/\!_{|D|} \cdot \Delta R = \Im \Delta L \tag{6}$$

where

$$\Im = \frac{\sqrt{2}}{|D| \cdot d_2}\sqrt{R^2\left(\frac{1}{\sin^2\gamma_1} + \frac{1}{\sin^2\gamma_2}\right) + \left(\frac{1}{\sin^2\gamma_3} + \frac{1}{\sin^2\gamma_4}\right)} \tag{7}$$

$\Im$ is the cumulative criterion, which includes both the geometrical factors (angles and distances) and the sensitivity of the ratio to the changes of A. It quantifies the influence of HOLZ line arrangements on the accuracy of the A measurement. The smaller $\Im$, the less is the error of A achievable at one and the same line position error. Thus, in the case of a *noise-free* CBED pattern, $\Im$ can be used as a criterion to select the incidence direction (zone axis) for the most accurate A determination. The $\Im$-criterion is not merely restricted to the ratio method, but can also be derived for other items used for comparison: areas, distances and angles. It is interesting to note that common practice [7,11,12] is to choose HOLZ lines crossing at an acute angle, as the shift of the crossing point (i.e. *sensitivity* of the ratio) is proportional to $1 / \sin(\gamma)$. Equation (7) indicates, however, that $\Im$ is also proportional to $1 / \sin(\gamma)$, i.e. the position of a HOLZ line intersection becomes less certain if the lines cross obliquely rather than at right angles. Thus, no real improvement in the accuracy can be achieved by choosing acute crossings.

Statistical error

To investigate the effect of noise, histograms of grey levels at the background region and along the maximum of the particular line were measured. Mean values μ_{bgr} and μ_{line} and standard deviations σ_{bgr} and σ_{line} were calculated. σ_{bgr} and σ_{line} were always observed to be approximately equal, so it was assumed that the noise σ was independent of the intensity. The SNR for each particular line was then defined as

$$\mathrm{SNR} = \frac{\mu_{\mathrm{line}} - \mu_{\mathrm{bgr}}}{\sigma} = \frac{S}{\sigma} \tag{8}$$

where S is a 'signal'. In the presence of noise there is a probability that, due to statistical variations in the pattern intensity, the Hough maximum is displaced from the 'true' position. The problem can be considered as follows: for given SNR, $\Delta\alpha$, $\Delta\rho$, width and length of a line, does the probability for the 'true' maximum to coincide with the measured one fall into a predefined confidence interval? For our purposes it will be more practical to solve the inverse task: to determine $\Delta\alpha$, $\Delta\rho$ (i.e. uncertainty of line parameters) for a predefined confidence interval. Below we will try to make reasonable assumptions about the form of the expression for noise-defined errors and then will fit the parameters of this formula by measuring simulated patterns.

Consider the pixel corresponding to the 'true' Hough maximum to have a signal I_0 and an adjacent pixel to have a signal I_1. Then, the null hypothesis for a t-test is $\Delta I = I_0 - I_1 = 0$ and the alternative for a 'one-tailed' test is that $\Delta I > 0$ (i.e. a 'true' pixel has a higher intensity then an adjacent one). The probability for ΔI can be written as

$$P = \mathrm{erf}\left(\frac{\Delta I}{\sigma_{\Delta I}}\right) \tag{9}$$

where $\sigma\Delta_I$ is the standard deviation of the statistical event ΔI. An accurate treatment would need a consideration of probabilities for all pixels within the region of the maximum. For simplicity, we will merely consider the probability that the measured maximum is displaced from the ideal position by a single pixel in either the α or ρ direction

$$P = \mathrm{erf}\left(\frac{\Delta I(\Delta\alpha)}{\sigma_{\Delta I}}\right) + \mathrm{erf}\left(\frac{\Delta I(\Delta\rho)}{\sigma_{\Delta I}}\right) \tag{10}$$

To determine ΔI we have to make assumptions about the second derivative at the maximum of a peak in Hough space. If we assume the HOLZ line to have a Gaussian profile $S \cdot \exp\left(-\frac{\rho^2}{2W^2}\right)$, then a cross section of the corresponding Hough peak through the maximum along the ρ-axis will be (assuming the origin to be at the peak maximum and expanding to Taylor series)

$$I(\rho) =$$
$$\int_{-L/2}^{L/2} S \cdot \exp\left(-\frac{\rho^2}{2W^2}\right) dl = LS \cdot \exp\left(-\frac{\rho^2}{2W^2}\right) \approx LS \cdot \left(1 - \frac{\rho^2}{2W^2}\right) \tag{11}$$

where l is the coordinate along the line, measured in pixels. The cross section of the Hough peak through the maximum along α-axis will then be, for small α

$$I(\alpha) =$$
$$\int_{-L/2}^{L/2} S \cdot \exp\left(-\frac{(l\sin(\alpha))^2}{2W^2}\right) dl \approx \int_{-L/2}^{L/2} S \cdot \exp\left(-\frac{l^2\alpha^2}{2W^2}\right) dw \approx LS\left(1 - \frac{L^2\alpha^2}{24W^2}\right) \tag{12}$$

Thus, ΔI for points adjacent to the maximum is

$$\Delta I(\Delta\rho) = \frac{LS\Delta\rho^2}{2W^2},\ \Delta I(\Delta\alpha) = LS\frac{L^2\Delta\alpha^2}{24W^2} \tag{13}$$

As the sampling intervals $\Delta\alpha$, $\Delta\rho$ for the Hough pattern can be chosen independently, $\Delta I(\Delta\alpha)$ can be set equal to $\Delta I(\Delta\rho)$, without loss of generality, by equating two expressions in eq. (13)

$$\Delta\rho^2 = L^2\Delta\alpha^2 / 12 \tag{14}$$

Substituting eqs (13) and (14) into eq. (10), we get

$$P = 2\mathrm{erf}\left(\frac{\frac{LS\Delta\rho^2}{2W^2}}{\sigma_{\Delta I}}\right) \tag{15}$$

The noise in Hough space σ_H is related to the noise in the image space σ by

$$\sigma_H = \sqrt{2L} \cdot \sigma \tag{16}$$

due to the fact that each point in Hough space is the sum of the image intensity along the line with the length L (in pixels), the factor 2 results from bilinear interpolation. Each point in Hough space corresponds to a slightly different fit to the line position and orientation and so consists of intersecting sets of pattern space pixels; thus, the noise in adjacent points of Hough space will be correlated. This fact means we cannot simply equate $\sigma_{\Delta I}$ to $\sqrt{2}\sigma_H$ as can be done for uncorrelated statistical values. The exact influence of noise correlation is difficult to predict. For $\Delta\rho$ tending to zero and for finite line length L, the following approximation can be made

$$\sigma_{\Delta I} \approx k\sigma\Delta\rho^a L^b \tag{17}$$

where a, b and k are parameters. Substitution of eq. (17) into eq. (15) results in

$$P = 2 \cdot \mathrm{erf}\left(\frac{L^{1-b}S\Delta\rho^{2-\alpha}}{k\sigma 2W^2}\right) \tag{18}$$

Applying the inverse erf function to both sides of eq. (18), shifting all the constants to one side and using the definition of SNR in eq. (8), we get

$$\mathrm{SNR}\frac{L^{1-b}\Delta\rho^{2-\alpha}}{W^2} = \mathrm{const} \tag{19}$$

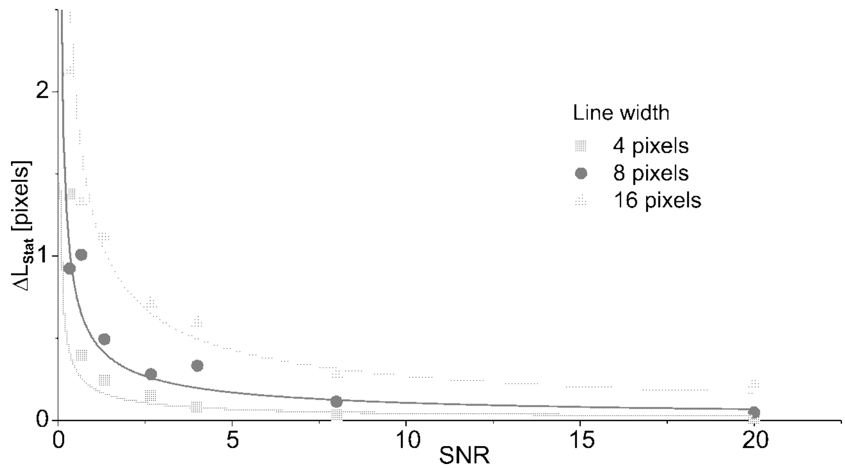

Fig. 2 Mean square deviations of the measured line position from the 'true' one plotted *vs* SNR (squares, circles and triangles represent different line-widths). The curves show the best-fit lines for eq. (21) for each line width. Curves represented are for $L = 600$.

Using the definitions of ΔL (eq. (1)) and $\Delta\alpha$ and $\Delta\rho$ (eq. (14)), ΔL can be expressed as

$$\Delta L \approx 0.5L\Delta\alpha + 0.5\Delta\rho \approx 2.2\Delta\rho \qquad (20)$$

Combining eqs (19) and (20) and making the substitutions $A = 1 / (2 - a)$ and $B = A / (1 - b)$, we can finally write for the uncertainty of the line position ΔL_{Stat} caused by the presence of the noise

$$\Delta L_{\text{Stat}} = K \cdot W^{2A} \cdot SNR^{-A} \cdot L^{B} \qquad (21)$$

Constant K includes the statistical confidence interval and A and B reflect the correlation of the noise in Hough space. To fit these parameters a grid of W, SNR and L data were generated and a set of 20 noisy images of a line was simulated for each data point on a grid. The standard deviation of the measured line position from the true one was used as ΔL_{Stat}.

Fitting of eq. (21) to simulated data results in $K = 0.66$, $A = 2/3$ and $B = -1/3$ (Fig. 2 shows the best fit curves for $L = 600$ pixels). Substituting these values into eq. (21) gives an expression for the statistical contribution to the error, SErr, in terms of the standard deviation (i.e. 50% confidence interval) of *measured* line position from the *true* one

$$\Delta L_{\text{Stat}} = 0.66 \cdot \sqrt[3]{\frac{W^4}{\text{SNR}^2 L}} \qquad (22)$$

It should be noted that eq. (22) reflects not the accuracy of the measurement method we propose, but a property of the line itself. If the position of a line is *defined* as the most probable position of its tip (which is the meaning of the Hough maximum), then ΔL_{Stat} in eq. (22) describes the uncertainty of a line position due to the noise *by definition*. By no means can the line be measured more accurately from a single image. The accuracy can be increased either by multiple measurements on *different* images (i.e. with different noise) or by assuming a line shape and fitting the whole profile.

The effect of only a finite number of gray levels was also studied and it was found that for the range of the conditions described (range of SNR, line width and length) sampling of a

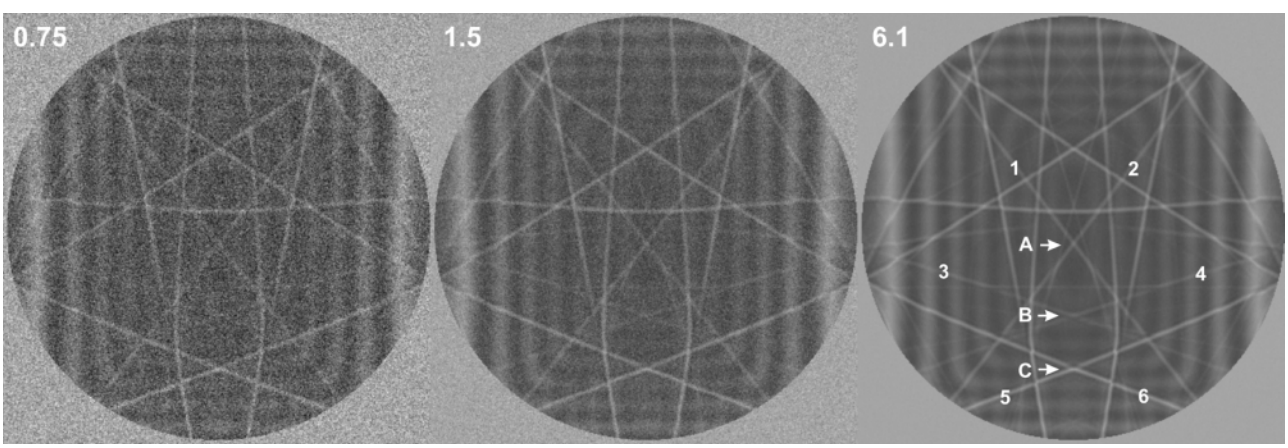

Fig. 3 Set of simulated CBED patterns with different amounts of applied noise. Patterns are background subtracted and inverted in contrast. Numbers mark lines involved in the measurement. The SNR value listed above each pattern is calculated for the line 1. A–C indicate crossing points used for the measurement.

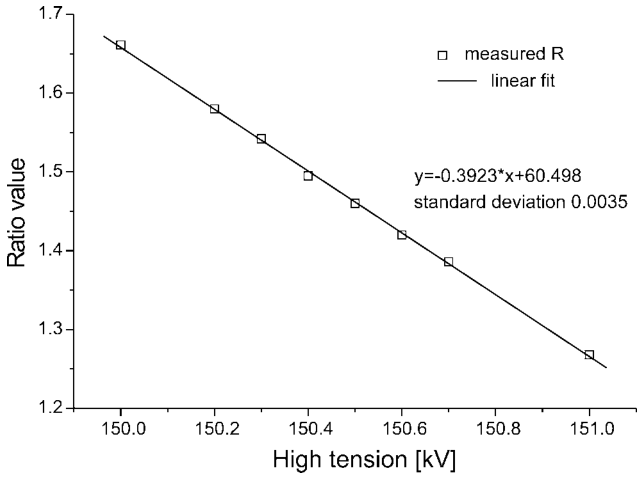

Fig. 4 Calibration curve measured with the use of noise-free simulated CBED patterns.

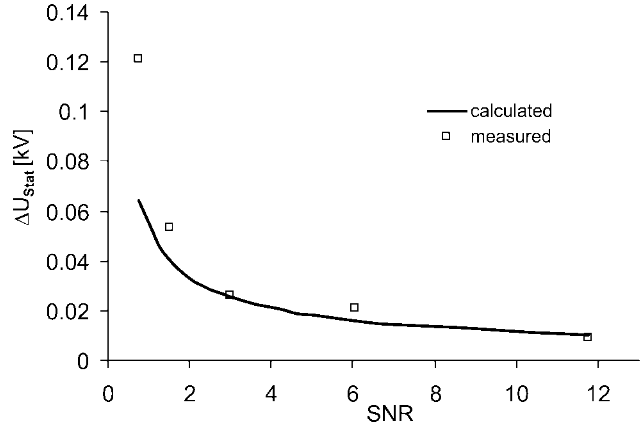

Fig. 5 Errors of high-tension measurement on simulated CBED patterns with different SNR (squares). The line presents the error prediction on the basis of eq. (24).

continuous intensity distribution to 16 grey levels and higher does not significantly influence the accuracy of the measurements.

Simulation test

To check the applicability of eq. (22), CBED patterns of [332] zone of Si for a high-tension range (150–151 kV) were simulated. Full dynamical Bloch wave calculations were performed with the program MBFIT [13]. Atomic scattering factors were calculated according to Doyle and Turner [14]. Lines of zeroth- to fourth-order Laue zones with g-values of <40 nm^{-1} were included and 113 beams were excited with maximum excitation error of 0.015 g. The radius of the CBED disc in reciprocal space was set to 10 nm^{-1} and the size of the simulated picture to 401×401 pixels.

The image with $U = 150.5$ kV was selected for a test. Random noise with Gaussian distribution was added to each pixel in the simulated pattern and the standard measurement procedure (ratio method) was applied to determine U. Figure 3 shows a row of such images with different SNRs (images are reversed in contrast and background subtracted). The lines used for the measurements are marked with numbers 1–6. The ratio $R = |AB| / |BC|$ was used to determine U. A calibration curve (Fig. 4) was obtained from noise-free simulated images. The GErr of the line positions was set to 0.025 pixels, which yields a GErr of the ratio (R) of 0.003. The standard deviation of measured R-values was 0.0035, which agrees well with the preset value of GErr. Taking the latter value as the error at a single point and using the slope of the calibration curve, -0.392 kV^{-1}, the accuracy of the calibration can be estimated to be ± 3 V.

Figure 5 shows the plot of the deviations of the measured values U (squares) from the 'true' 150.5 kV *vs* SNR. The deviations were averaged over 20 images for each SNR value and each of the images for a given SNR had a different simulated noise pattern. The SNR values indicated in Fig. 5 are the values for line 1. To check the validity of eq. (22) it was modified to

$$\Delta L_{\mathrm{Stat}} = \sigma^{\frac{2}{3}}\, 0.66 \cdot \sqrt[3]{\frac{W^4}{S^2 L}} = \sigma^{\frac{2}{3}} \Delta L_{\mathrm{Sens}} \qquad (23)$$

where ΔL_{Sens} includes only the parameters of the line and reflects the sensitivity of position of the particular line to the noise. Substituting ΔL_{Stat} for each line to eq. (3), we get for SErr of the high-tension determination

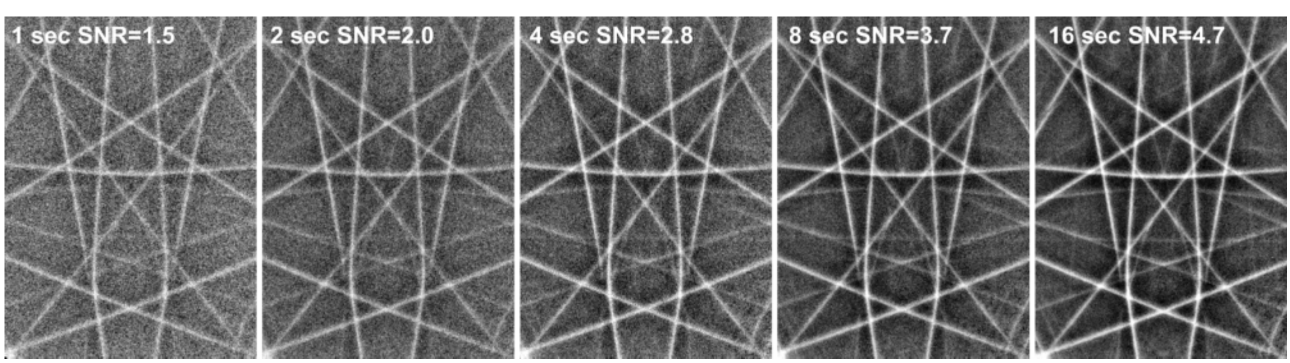

Fig. 6 Experimental CBED patterns of [332] zone of Si obtained with different exposure times at the nominal 150 kV. The SNR indicated is for the line 1, as in Fig. 3. A 1 K × 1 K CCD camera (Gatan) was used to acquire the patterns.

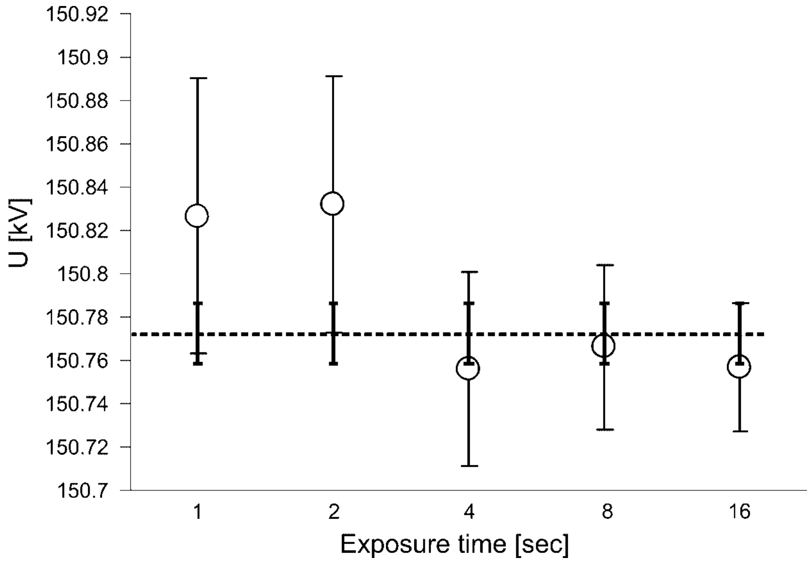

Fig. 7 Measured accelerating voltage for different patterns (Fig. 6) with corresponding calculated statistical errors. The dashed line represents the weighted mean of all five measurements and the corresponding error.

$$\Delta U_{\mathrm{Stat}} = \Delta A_{\mathrm{Stat}} = \frac{\sigma^{\frac{2}{3}}}{|D|}\Delta R_{\mathrm{Sens}} = \Re\sigma^{\frac{2}{3}} \tag{24}$$

Here, $\Re$ includes the geometry of the line arrangement as well as line intensities and widths, and reflects the robustness of particular HOLZ line arrangement to the noise. For each line (lines 1–6, Fig. 3) its intensity, width and length were measured and $\Re$ was calculated for the ratio $|AB| / |BC|$. The resulting curve for the *calculated* SErr of U measurement (eq. (24)) is plotted as Fig. 5. It is seen that the *measured* standard deviation of U is in good agreement with ΔU_{Stat} *predicted* by eq. (24) for a reasonable range of SNR. For SNR less than unity, SErr is strongly underestimated due to simplifications of the statistical model. However, the absolute values of the errors for this SNR range are too high to consider such noisy images to be of practical value.

Experimental example

Experimental CBED patterns of [332] zone of Si were recorded with JEM-3010 (LaB_6) at nominal high-tension of 150 kV at room temperature. Variation of the exposure time from 1 to 16 s allowed the creation of patterns with different SNRs. A row of such images (contrast inverted and background subtracted) is presented in Fig. 6; the SNR for line 1 (compare with Fig. 3) is indicated. As for the case of the simulated CBED patterns, the ratio $R = |AB| / |BC|$ was measured and the high tension was determined by using the calibration curve shown in Fig. 4. Table 1 gives the summary of the measured and calculated quantities for each pattern. Figure 7 represents the measured accelerating voltage with the corresponding calculated (eq. (24)) SErrs for each pattern. As can be seen, all measurements have overlapping error intervals. The weighted mean of the measurements was calculated to be 150.772 kV. This value falls within the error intervals of all the measurements. The estimated error of weighted mean is as low as 14 V.

Concluding remarks

We have analyzed thoroughly the accuracy limitations of the lattice parameter determination by CBED, which are related to the procedure of HOLZ line position measurement. A method of line position measurement based on Hough transformation was introduced, which permits the measurement errors to be reduced to arbitrarily small values. However, it has been shown that the presence of the noise on experimental images sets the principal limit for the accuracy. A formula for the noise-limited uncertainty of a line position has been derived. Furthermore, this approach has been extended for the full set of HOLZ lines, used for lattice parameter determination, resulting in a cumulative $\Re$-criterion. This criterion reflects the robustness of a particular HOLZ line geometry to the noise in the sense of the final measurement accuracy. It can be used

Table 1. Measured and calculated quantities for each pattern

Exposure time [s]	Signal (line 1) [a.u.]	Noise [a.u.]	SNR (line 1)	ΔL_{Stat} (line 1) [pixel]	Calculated ΔU [kV]	Determined U [kV]
1	40.4	27.0	1.5	0.37	0.064	150.826
2	81.9	40.7	2.0	0.34	0.059	150.832
4	155.8	55.0	2.8	0.27	0.045	150.756
8	314.4	85.8	3.7	0.22	0.038	150.766
16	647.7	138.1	4.7	0.18	0.030	150.757

for a priori estimation of the best accuracy obtainable for each particular CBED pattern as well as for the selection of the best experimental parameters (incidence direction, HOLZ lines involved).

The approach has been evaluated with the use of simulated and experimental CBED patterns, demonstrating a good estimation for the error of the measured value in the range of experimentally reasonable SNRs. It was shown that even for the case of a CBED pattern recorded with a LaB_6 cathode, at room temperature and without energy filtering, the relative precision of 2×10^{-4} can be obtained from a single measurement. The use of a cooling stage as well as an energy filter to remove inelastic background should result in much better accuracy. However, in these cases other limiting factors than the noise may occur, which then should be considered as well.

The a priori knowledge of the measurement error permits an increase in the precision by a factor of about $\sqrt{N}$, by averaging a number of N-values obtained with different ratios from one and the same CBED pattern, if (and only if) all these values are within the measurement error. If not, then it must be concluded that the model of strain used in the simulations is not correct.

Acknowledgments

The authors are indebted to Dr Alasdair Preston for valuable remarks and careful reading of the manuscript and thank Dr Svetlana Cherepanova for discussions. The work has been supported by the Deutsche Forschungsgemeinschft Ri 607/1-1.

References

1 Zuo J M, Kim M, and Holmestad R J (1998) A new approach to lattice parameter measurements using dynamical electron diffraction and pattern matching. *J. Electron Microsc.* **47**: 121–127.

2 Rozeveld S J and Howe J M (1993) Determination of multiple lattice parameters from convergent-beam electron diffraction patterns. *Ultramicroscopy* **50**: 41–56.

3 Wittman R, Parzinger C, and Gerthen D (1998) Quantitative determination of lattice parameters from CBED patterns: accuracy and performance. *Ultramicroscopy* **70**: 145–159.

4 Kramer S, Mayer J, Witt C, Weikenmeier A, and Ruhle M (2000) Analysis of local strain in aluminium interconnects by energy filtered CBED. *Ultramicroscopy* **81**: 245–262.

5 Wakayama Y, Takahashi Y, and Tanaka S (1997) Convergent beam electron diffraction measurement for local strain distribution in Si around $NiSi_2$ island. *Jpn. J. Appl. Phys.* **36**: 5072–5078.

6 Kaiser U, Saitoh K, Tsuda K, and Tanaka M (1999) Application of the CBED method for the determination of lattice parameters of cubic SiC films on 6H SiC substrates. *J. Electron Microsc.* **48**: 221–233.

7 Yonemura M, Sueoka K, and Kamei K (2000) Effect of heavy boron doping on the lattice strain around platelet oxide precipitates in Czochralski silicon wafers. *J. Appl Phys.* **88**: 503–507.

8 Rossouw C and Venkatesan K (2001) HOLZ line analysis of lattice parameters in Mg alloys. *J. Electron Microsc.* **50**: 391–404.

9 Kraemer S and Mayer J (1999) Using the Hough transform for HOLZ line identification in convergent beam electron diffraction. *J. Microsc* **194**: 2–11.

10 Hough P V C (1962) *A Method and Means for Recognizing Complex Patterns*. US Patent no. 3.069.654.

11 Okuyama T, Nakayama M, Sadamitsu S, Nakashima J, and Tomokiyo Y (1997) Analysis of local lattice strains around plate-like oxygen precipitates in Czochralski-silicon wafers by convergent beam electron diffraction. *Jpn. J. Appl. Phys.* **36**: 3359–3365.

12 Toda A, Ikarashi N, and Ono H (2000) Local lattice strain measurements in semiconductor devices by using convergent-beam electron diffraction. *J. Cryst. Growth* **210**: 341–345.

13 Tsuda K and Tanaka M (1995) Refinement of crystal structure parameters using convergent-beam electron diffraction: the low temperature phase of $SrTiO_3$. *Acta Cryst.* **A51**: 7–19.

14 Doyle P A and Turner P S (1968) Relativistic Hartree–Fock X-ray and electron scattering factors. *Acta Cryst.* **A24**: 390–397.